Improved Test of Time Dilation in Special Relativity

G. Saathoff,[1] S. Karpuk,[2] U. Eisenbarth,[1] G. Huber,[2] S. Krohn,[1] R. Muñoz Horta,[1] S. Reinhardt,[1] D. Schwalm,[1] A. Wolf,[1] and G. Gwinner[1]

[1]*Max-Planck-Institut für Kernphysik, 69029 Heidelberg, Germany*
[2]*Institut für Physik, Universität Mainz, 55099 Mainz, Germany*

(Received 24 June 2003; published 4 November 2003)

An improved test of time dilation in special relativity has been performed using laser spectroscopy on fast ions at the heavy-ion storage-ring TSR in Heidelberg. The Doppler-shifted frequencies of a two-level transition in $^7Li^+$ ions at $v = 0.064c$ have been measured in the forward and backward direction to an accuracy of $\Delta\nu/\nu = 1 \times 10^{-9}$ using collinear saturation spectroscopy. The result confirms the relativistic Doppler formula and sets a new limit of 2.2×10^{-7} for deviations from the time dilation factor $\gamma_{SR} = (1 - v^2/c^2)^{-1/2}$.

DOI: 10.1103/PhysRevLett.91.190403 PACS numbers: 03.30.+p, 06.30.Ft, 42.62.Fi

The core of special relativity (SR) as a theory of local spacetime is Lorentz invariance, which is one of the most fundamental symmetries of all modern descriptions of nature. Because of this fundamental role there is much interest in experimental tests of SR, in particular, as violations of this symmetry have been considered in unification theories combining the standard model of particle physics with gravity [1].

Any deviation from SR would violate the Einstein relativity principle causing effects, which are dependent on the choice of the reference frame. Following Robertson [2], Mansouri and Sexl (MS) [3] developed a kinematical test theory assuming generalized Lorentz transformations between a hypothetical preferred-frame $\Sigma(T, \vec{X})$ and a frame $S(t, \vec{x})$ moving at a velocity $\vec{V}$ along X relative to Σ, which read, using Einstein synchronization,

$$T = \Gamma\left(\frac{t}{\hat{a}} + \frac{Vx}{\hat{b}\,c^2}\right); \tag{1}$$

$$X = \Gamma\left(\frac{x}{\hat{b}} + \frac{Vt}{\hat{a}}\right); \qquad Y = \frac{y}{\hat{d}}; \qquad Z = \frac{z}{\hat{d}},$$

with $\Gamma = (1 - V^2/c^2)^{-1/2}$ and c being the speed of light in Σ. This model, which is commonly used to quantify the sensitivity of an experiment to violations of SR, contains three velocity-dependent test functions $\hat{a}(V^2)$, $\hat{b}(V^2)$, and $\hat{d}(V^2)$, which modify time dilation as well as Lorentz contraction in longitudinal and transverse direction. For SR, they reduce to $\hat{a}(V^2) = \hat{b}(V^2) = \hat{d}(V^2) = 1$. Expanding these functions in powers of V^2/c^2, i.e., $\hat{a}(V^2) = [1 + \hat{\alpha}V^2/c^2 + \mathcal{O}(c^{-4})]$, $\hat{b}(V^2) = [1 + \hat{\beta}V^2/c^2 + \mathcal{O}(c^{-4})]$, and $\hat{d}(V^2) = [1 + \hat{\delta}V^2/c^2 + \mathcal{O}(c^{-4})]$, one is left with three test parameters $\hat{\alpha}$, $\hat{\beta}$, and $\hat{\delta}$. The experiments which allow one to fix these parameters are the Ives-Stilwell (IS) experiment [4], which measures $\hat{\alpha}$, the Michelson-Morley (MM) experiment [5] measuring the parameter combination $|\hat{\beta} - \hat{\delta}|$, and the Kennedy-Thorndike (KT) experiment [6] sensitive to $|\hat{\alpha} - \hat{\beta}|$. Modern versions of the MM [7] and the KT experiment [8], where the preferred frame Σ is identified with the CMB system, in which the 3 K cosmic microwave background is isotropic and in which the Earth-bound laboratory system S_{lab} is moving with a velocity of $V_{lab} \approx 350$ km/s, have recently led to improved limits of $|\hat{\beta} - \hat{\delta}| \leq 1.5 \times 10^{-9}$ [9] and $|\hat{\alpha} - \hat{\beta}| \leq 6.9 \times 10^{-7}$ [10], rendering, at present, the IS test of $\hat{\alpha}$ the least accurate.

In the original IS experiment [4] hydrogen atoms in canal rays are used as clocks moving at a velocity $\beta = v/c = 0.005$ with respect to S_{lab}. Time dilation is tested by measuring the Doppler-shifted frequencies ν_p and ν_a of the Hβ line in parallel ($\vartheta_p = 0$) and antiparallel ($\vartheta_a = \pi$) direction with respect to $\vec{\beta}$. Within SR the respective Doppler shifts are given by the relativistic Doppler formula, $\nu_0 = \gamma_{SR}(\beta^2)(1 - \beta\cos\vartheta_{p,a})\nu_{p,a}$, where ν_0 is the transition frequency in the system S_{rest}, in which the hydrogen atom is at rest. Multiplication of these equations yields the velocity-independent relation $\nu_p\nu_a = \nu_0^2$, since the SR time dilation factor $\gamma_{SR}^2(\beta^2)$ obeys $\gamma_{SR}^2(\beta^2) \times (1 - \beta^2) = 1$. A detailed analysis of the experiment within the MS test theory has been carried out in [11] and shows that a nonvanishing test parameter $\hat{\alpha}$ would modify the outcome of the IS experiment as

$$\frac{\nu_p\nu_a}{\nu_0^2} = 1 + 2\,\hat{\alpha}\,(\beta^2 + 2\,\vec{\beta}_{lab} \cdot \vec{\beta}) + \mathcal{O}(c^{-4}), \tag{2}$$

with $\vec{\beta}_{lab} = \vec{V}_{lab}/c$. Note that the result is independent of the actual synchronization procedure as well as on $\hat{\beta}$ and $\hat{\delta}$; moreover, the β^2 term allows one to determine $\hat{\alpha}$ absolutely without having to rely on the precise knowledge of β_{lab} (at least as long as β is larger than β_{lab}), while the $2\vec{\beta}_{lab} \cdot \vec{\beta}$ term gives access to $\hat{\alpha}$ via sidereal modulations. The original IS experiment provided an absolute upper bound of $\hat{\alpha} < 1 \times 10^{-2}$. Later, significant improvements have been achieved using laser techniques instead of conventional spectrometers [12]; two-photon spectroscopy on a $\beta = 0.0036$ neon atomic beam has set an absolute bound of $\hat{\alpha} < 2.3 \times 10^{-6}$ [13] and even $\hat{\alpha} < 1.4 \times 10^{-6}$ [14] from the limit on sidereal variations.

A further improvement of this limit has been made possible by the development of heavy-ion storage rings like the TSR in Heidelberg [15], which provide high-quality particle beams at a considerably higher velocity. The present experiment uses $^7Li^+$ ions stored in the TSR at a velocity of $\beta = 0.064$ (13.3 MeV). The triplet spectrum of the heliumlike $^7Li^+$ has a convenient optical transition $2s\,^3S_1 \rightarrow 2p\,^3P_2$ at 548.5 nm with a well resolved and precisely known fine and hyperfine structure multiplet. A first version of this experiment employed collinear optical-optical double resonance spectroscopy on a Λ-type three-level system and has set the hitherto best absolute bound of $\hat{\alpha} < 8 \times 10^{-7}$ [16]. Experimentally, the technique was limited by the large observed linewidth of the Λ resonance of almost 60 MHz, compared to a natural width of 3.8 MHz. Time-resolved studies of the Λ system during the present experiment have now revealed that most of this broadening is caused by velocity changes between subsequent excitations of the two transitions of the Λ system. The underlying reason is that Λ spectroscopy does not require a *simultaneous* interaction of both lasers with an ion.

To avoid this problem, the present experiment uses collinear saturation spectroscopy on the closed two-level system of rest frame frequency ν_0 formed by the $^3S_1(F = 5/2) \rightarrow {}^3P_2(F = 7/2)$ transition in $^7Li^+$. The laboratory frequencies ν_p and ν_a of the parallel and antiparallel laser beams must obey relation (2) for resonance, which is indicated by a Lamb dip in the fluorescence spectrum. In contrast to the previous measurement, saturation spectroscopy requires the simultaneous interaction of both lasers with an individual ion, the simultaneity being defined by the spontaneous decay time of the excited state of 43 ns. This time is much shorter than any time scale connected with velocity-changing processes in the ring.

The 13.3 MeV ion beam is provided by a tandem Van de Graaff accelerator. Starting with negative Li ions, about 10% of the ions emerge from the gas stripper in the metastable $^3S_1$ state. Typically 10^8 ions are injected into the TSR and kept on a closed orbit of 55.4 m circumference, the lifetime of the metastable fraction of the ion beam being about 13 s. To prepare a high-quality ion beam, electron cooling is applied to the beam after injection. At equilibrium, which is reached after about 5 s of cooling, the ion beam in the ion-laser interaction region (see Fig. 1) has a σ width of $\approx 250\ \mu$m, a σ divergence of $\approx 50\ \mu$rad, and a longitudinal momentum spread of $\sigma_p/p = 3.5 \times 10^{-5}$. The latter leads to a Doppler width of the transition of about 2.5 GHz (FWHM), which is much smaller than the hyperfine (hfs) splittings of the involved levels [16]. Moreover, the ion beam is moderately bunched with the 3rd harmonic of the average revolution frequency. By controlling the bunching frequency, the mean ion velocity can be fine adjusted such that the two-level transition is tuned into resonance with a copropagating Ar^+ laser beam at $\lambda_p = 514.7$ nm exactly for ions in the center of the velocity

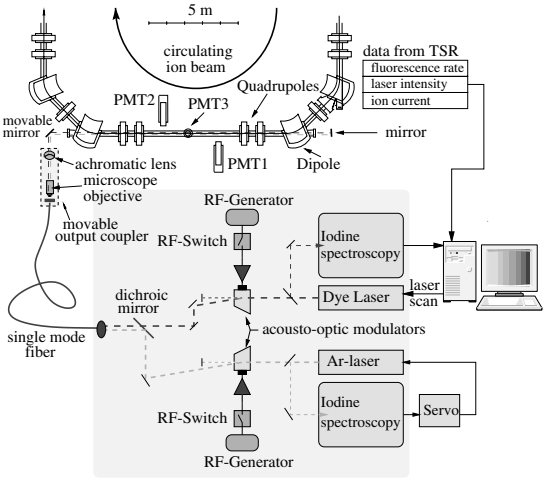

FIG. 1. Setup of the experiment at the ion storage ring TSR.

distribution. The corresponding resonance wavelength of the counterpropagating light is $\lambda_p = 584.7$ nm and is provided by a single-mode dye laser.

The Ar^+ laser (Lexel 85-1) is first locked to a high-finesse Fabry-Perot interferometer (Tec Optics, SA300) via a piezo-driven mirror in order to compensate for short-term fluctuations. The laser is frequency modulated at 29 kHz with a modulation amplitude of 2 MHz, and saturation spectroscopy in I_2 is performed in an external cell stabilized at a temperature of $6 \pm 0.1\,^\circ$C. 1st harmonic lock-in detection is used to lock the FPI to the a_3 hfs component of the P(13)43-0 line. The frequency uncertainty of the Ar^+ laser is composed of the uncertainty of the a_3 component [17] (1.5 kHz), residual Doppler background due to a small angle between saturation and probe beam (50 kHz), and the deviation of the iodine cell temperature from the recommended temperature of $-5\,^\circ$C (35 kHz); the uncertainty amounts in total to 61 kHz.

The dye laser (Coherent 699-21) has a linewidth of below 1 MHz and is scanned across the $^7Li^+$ resonance, typically over a range of 200 MHz. In order to determine the frequency of the scanning laser, a suitable $^{127}I_2$ hfs line is recorded simultaneously by saturation spectroscopy in a second external cell stabilized to $6 \pm 0.3\,^\circ$C. The laser is frequency modulated at 36 kHz with a modulation amplitude of 2 MHz and the iodine line is detected with the 1st harmonic lock-in technique. The closest iodine line, the *a* component of P(10)14-1, is 60 MHz lower in frequency than the expected position of the Lamb dip. To minimize the error in the frequency calibration, the dye as well as the Ar^+ laser beam going into the TSR are passed through acousto-optic frequency shifters in order to shift the Lamb dip very close to the frequency of the I_2 line, which has been calibrated to the acousto-optically shifted *i* component of R(99)15-1 known from a previous calibration run [18].

The two laser beams are merged with a dichroic mirror and guided to the TSR by a single-mode

polarization-maintaining fiber. The bichromatic laser beam is then directed via an achromatic telescope through the experimental section of the TSR and retroreflected by a flat mirror behind the experimental section with the laser foci placed close to the mirror. First the dye laser beam is merged with the ion beam using stepmotorized translation and rotation stages. To monitor the overlap, the Ar^+ laser is blocked, and the dye laser is tuned into resonance for ions in the center of the velocity distribution. The laser beam is then precisely shifted in parallel horizontally as well as vertically, and the fluorescence rates are recorded by three photomulipliers located at different positions along the experimental section (see Fig. 1). By observing the simultaneous occurrence of the maxima of the fluorescence signals in the three photomultipliers as a function of the horizontal and vertical displacement, the parallelity of the laser to the ion beam could be assured and frequently checked during the experiment to better than 70 μrad. Then the Ar^+ laser beam is overlapped with the dye laser by placing an aperture around the bichromatic laser beam in front of the TSR entrance window and centering the reflected beam back through this aperture, thus achieving also a radial laser-laser angle accuracy of better than 70 μrad.

The measurement then proceeds as follows: After an injection the ion beam is first electron-cooled for 5 s before the lasers are turned on and the fluorescence rate is recorded as a function of the dye laser frequency. Figure 2 shows a run reflecting 82 laser scans, each spanning 200 MHz in steps of 1 MHz. To eliminate slow frequency drifts of the dye laser, the zero point of the frequency scale of each laser scan is individually adjusted by a fit to the iodine line before the scans are added up. Moreover, as the limited lifetime of the metastable ions in the TSR leads to a decrease of the fluorescence background during a laser scan, the laser scan cycles, each consisting of 200 laser steps of 100 ms, are decoupled from the ion injection cycles by injecting a new beam after 46 consecutive laser steps; by adding up a sufficiently large number of scans the ion beam decay thus averages out. At each laser step the fluorescence rate is measured at three different laser beam configurations and stored in three seperate spectra. One, taken with both lasers interacting with the ions simultaneously, contains the Doppler background together with the Lamb dip [curve (*b*) in Fig. 2]. Two additional spectra are recorded with the two lasers applied separately, the sum of which reflects the Doppler-background alone [curve (*a*)] and, subtracted from (*b*), leads to the pure Lamb dip spectrum (*c*). To record the three fluorescence rates quasisimultaneously, the acousto-optic modulators are switched such that the laser beam configurations are changed every 200 μs.

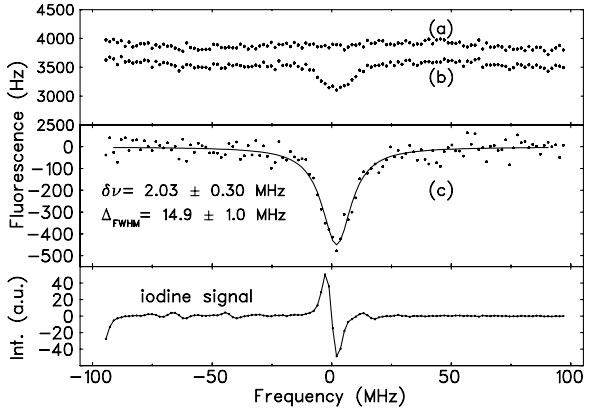

FIG. 2. Fluorescence signal observed with PMT3 for a multiple scan of the Lamb dip. Spectrum (b) is taken with both lasers interacting with the ions simultaneously. Spectrum (a), plotted with an offset for clarity, is the sum of the spectra taken with the lasers applied separately and reflects the Doppler background. The pure Lamb dip spectrum (c) is obtained by subtracting (a) from (b). The zero of the frequency scale corresponds to the position of the P(10)14-1 *a* component.

A series of Lamb dips was recorded at different total laser intensities in order to investigate possible intensity-dependent frequency shifts, matching carefully the intensities of the two lasers to balance the laser forces on the ions. The Lamb dip center frequency $\delta\nu$ with respect to the iodine line and its width are determined by a fit of the pure Lamb dip spectra with a Lorentzian line shape, which represents the measured dips very well. An extrapolation of the measured saturation-broadened linewidths to zero intensity gives ≈ 11 MHz (FWHM), which is 7 MHz in excess of the natural width. This excess can be attributed to the modulation of the two lasers and, to a lesser degree, to the Zeeman effect caused by residual magnetic fields in the experimental section, which — as we use linearly polarized light — is expected to cause only a broadening but no net shift. In Fig. 3 the Lamb dip center frequency $\delta\nu$ of the Lamb dip is plotted versus the sum intensity, which is varied over 1 order of magnitude. A slight dependence of about 3 MHz over the whole intensity range is found, which we attribute to local changes in the velocity distribution caused by the laser forces. These changes modify the Doppler background and lead to distortions of the Lamb dip. As we subtract the Doppler background measured alternatively with the signal at 5 kHz, distortions of the Lamb dip occurring on this time scale should cancel in the difference spectrum.

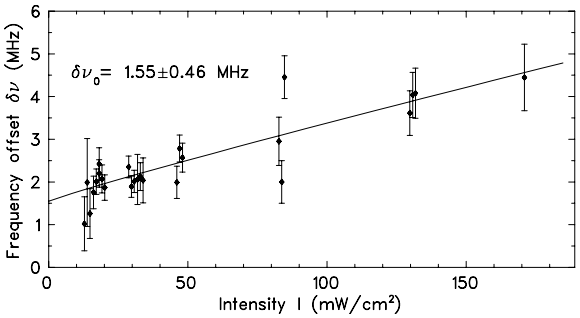

FIG. 3. Frequency offset of the Lamb dip from the I_2 reference line as a function of the total laser intensity.

TABLE I. Accuracy budget of the saturation spectroscopy.

	Frequency (kHz)	1σ error (kHz)
Experimental result:		
Iodine reference line $\nu_{\text{a-comp}}$	512 671 028 023	152
AOM shift (dye laser) $\delta\nu_{\text{dye}}^{\text{AOM}}$	414 000	negl.
Lamb dip offset to reference $\delta\nu_{\text{L}}$	1 550	460
Wave front corr. (dye laser) $\delta\nu_{\text{dye}}^{\text{wf}}$	−665	160
Laser-laser angle		40
Laser-ion angle		10
Ion beam divergence		50
Frequency calibration		50
Total $\nu_{\text{a}}^{\text{exp}}$	512 671 442 908	517
Prediction from SR:		
Ar^+ laser frequency ν_{Ar}	582 490 603 442	61
AOM shift (Ar^+ laser) $\delta\nu_{\text{Ar}}^{\text{AOM}}$	−400 000	negl.
Wave front corr. (Ar^+ laser) $\delta\nu_{\text{Ar}}^{\text{wf}}$	+179	70
$^7Li^+$ rest frequency ν_0 [20]	546 466 918 790	400
Total $\nu_{\text{a}}^{\text{SR}}$	512 671 443 186	755

However, a locally distorted velocity distribution also influences the frequency of the resonance through the ac-Stark shift [19], and this effect is not canceled by the subtraction scheme. While the ac-Stark shift scales linearly with intensity for a given velocity distribution, the latter is also intensity dependent. We therefore extrapolate the resonance frequency to zero intensity by fitting $\delta\nu = \delta\nu_{\text{L}} + mI^{\kappa}$ with m, κ, and $\delta\nu_{\text{L}}$ as fit parameters, yielding an almost linear dependence ($\kappa = 0.93$) with a frequency offset at intensity zero of $\delta\nu_{\text{L}} = 1550 \pm 460$ kHz.

Deviations of the laser-ion angles ϑ_{p} and ϑ_{a} from 0 and π cause frequency shifts. Assuming plane-wave light, we find $\Delta\nu_{\text{a}}/\nu_{\text{a}} = -\beta\vartheta_{\text{p}}^2/2(1-\beta)$ in the case of one misaligned laser ($\vartheta_{\text{a}} = \pi$, $\vartheta_{\text{p}} \neq 0$), and $\Delta\nu_{\text{a}}/\nu_{\text{a}} = -\vartheta_{\text{p}}^2\beta^2$ for both lasers mutually aligned, but tilted against the ion beam ($\vartheta_{\text{p}} = \pi - \vartheta_{\text{a}} \neq 0$). Alignment uncertainties of 70 μrad for both the laser-ion and laser-laser angles result in frequency uncertainties of $\Delta\nu_{\text{a}} = 10$ kHz and $\Delta\nu_{\text{a}} = 40$ kHz, respectively. The frequency error due to the divergence of the electron-cooled ion beam amounts to less than 50 kHz. On the other hand, a Gaussian laser beam profile has a phase deviation $\xi(z) = \arctan z/z_{\text{R}}$ from a plane wave in the direction of the optical axis z, where z_{R} denotes the Rayleigh range and $z = 0$ the focal point. For a particle traveling along z with velocity v, this phase change results in a frequency shift of $\delta\nu^{\text{wf}} = v\mathrm{d}\xi(z)/\mathrm{d}z$. From the measured position of the foci and the Rayleigh ranges of both lasers, the shifts are estimated by a Monte-Carlo simulation to $\delta\nu_{\text{Dye}}^{\text{wf}} = (-665 \pm 160)$ kHz for the dye laser and $\delta\nu_{\text{Ar}}^{\text{wf}} = (179 \pm 70)$ kHz for the Ar^+ laser.

Taking all systematic errors into account, the result of the frequency measurement of the Lamb dip (see Table I) reads $\nu_{\text{a}}^{\text{exp}} = 512\,671\,442\,908 \pm 517$ kHz. This has to be compared to the prediction from SR $\nu_{\text{a}}^{\text{SR}} = \nu_0^2/(\nu_{\text{Ar}} + \delta\nu_{\text{Ar}}^{\text{AOM}} + \delta\nu_{\text{Ar}}^{\text{wf}}) = 512\,671\,443\,186 \pm 755$ kHz. The difference between these values $\Delta = \nu_{\text{a}}^{\text{exp}} - \nu_{\text{a}}^{\text{SR}} = -278 \pm 915$ kHz is compatible with zero within the 1 σ error and results in an improved absolute upper limit for $\hat{\alpha}$ of

$$\hat{\alpha} < 2.2 \times 10^{-7} \tag{3}$$

assuming $\beta \gg \beta_{\text{lab}}$. Note, that the present accuracy of the rest frequency ν_0, which enters Eq. (2) in quadrature, dominates the overall accuracy and needs to be improved for further progress. But already now the storage-ring method improves the absolute (i.e., preferred-frame independent) limit for deviations of the time dilation factor from SR by one order of magnitude compared to other measurements.

Helpful discussions with M. Weidemüller and technical support by M. Grieser, K. Horn, and H. Krieger are gratefully acknowledged.

[1] D. Colladay and V. A. Kostelecký, Phys. Rev. D **58**, 116 002 (1998).
[2] H. P. Robertson, Rev. Mod. Phys. **21**, 378 (1949).
[3] R. Mansouri and R. U. Sexl, Gen. Relativ. Gravit. **8**, 497 (1977); **8**, 515 (1977); **8**, 809 (1977).
[4] H. E. Ives and G. R. Stilwell, J. Opt. Soc. Am. **28**, 215 (1938).
[5] A. A. Michelson and E. W. Morley, Am. J. Sci. **34**, 333 (1887).
[6] R. J. Kennedy and E. M. Thorndike, Phys. Rev. **42**, 400 (1932).
[7] A. Brillet and J. L. Hall, Phys. Rev. Lett. **42**, 549 (1979).
[8] D. Hils and J. L. Hall, Phys. Rev. Lett. **64**, 1697 (1990).
[9] H. Müller *et al.*, Phys. Rev. Lett. **91**, 020401 (2003).
[10] P. Wolf *et al.*, Phys. Rev. Lett. **90**, 060402 (2003).
[11] M. Kretzschmar, Z. Phys. A **342**, 463 (1992).
[12] J. J. Snyder and J. L. Hall, in *Lecture Notes in Physics*, edited by S. Haroche *et al.* (Springer, New York, 1975), Vol. 43.
[13] R. W. McGowan *et al.*, Phys. Rev. Lett. **70**, 251 (1993).
[14] E. Riis *et al.*, Phys. Rev. Lett. **60**, 81 (1988).
[15] D. Habs *et al.*, Nucl. Instrum. Methods Phys. Res., Sect. B **43**, 390 (1989).
[16] R. Grieser *et al.*, Appl. Phys. B **59**, 127 (1994).
[17] R. J. Jones *et al.*, Appl. Phys. B **74**, 597 (2002).
[18] R. Grieser *et al.*, Z. Phys. A **348**, 147 (1994).
[19] C. Cohen-Tannoudji, Ann. Phys. (Paris) **7**, 423 (1962).
[20] E. Riis *et al.*, Phys. Rev. A **49**, 207 (1994). In addition to ν_0, they determined the fine and hyperfine spittings, which agree well with theory and a recent measurement by J. J. Clarke and W. A. van Wijngaarden, Phys. Rev. A **67**, 012506 (2003). A further measurement by H. Rong *et al.* [Z. Phys. D **25**, 337 (1993); Eur. Phys. J. D **3**, 217 (1998)] shows a substantial disagreement in fs and hfs of up to 9σ and a 2σ deviation of 2.3 MHz in ν_0. Hence we adopt the value of Riis.